# Microfabricated strained substrates for Ge epitaxial growth

P. G. Evans,[a] P. P. Rugheimer, and M. G. Lagally
*Department of Materials Science and Engineering and Materials Science Program, University of Wisconsin, Madison, Wisconsin 53706*

C. H. Lee[b] and A. Lal[c]
*Department of Electrical and Computer Engineering, University of Wisconsin, Madison, Wisconsin 53706*

Y. Xiao, B. Lai, and Z. Cai
*Advanced Photon Source, Argonne National Laboratory, Argonne, Illinois 60439*

(Received 29 December 2004; accepted 27 February 2005; published online 28 April 2005)

The manipulation of strain in micromachined silicon structures presents an opportunity in the control of surface processes in epitaxial growth. With appropriate fabrication techniques, the magnitude, crystallographic direction, and symmetry of the strain at a Si surface can be precisely controlled with this strategy. Synchrotron x-ray microdiffraction techniques allow simultaneous independent measurements of the strain and bending in these structures and serve to calibrate the fabrication process. Bending is the dominant source of strain in a microfabricated Si bridge loaded at its ends by silicon nitride thin films that we have used as a strained substrate in studies of Ge epitaxial growth. The total strain difference between the top and bottom of the bent bridge exceeds $10^{-3}$ in present structures and can potentially be increased in optimized devices. These micromachined substrates complement other methods for producing strained silicon and silicon–germanium structures for improved electrical device performance and for fundamental studies of epitaxial growth. © *2005 American Institute of Physics*. [DOI: 10.1063/1.1894579]

## I. INTRODUCTION

The development of silicon-on-insulator (SOI) for electronic device fabrication is based on the finite thickness of the thin top template layer of Si and offers increases in device performance not easily achievable on bulk Si substrates. Recent advances in SOI wafer fabrication suggest that SOI substrates with strained Si template layers (SSOI) will soon be widely available.[1,2] The strain in these layers can be as large as a few percent, offering additional increases in device performance compared to unstrained Si.[3,4] This strain has a wide range of physical effects, however, including the potential to modify epitaxial film growth, in which the diffusion of adatoms on the surface has an important role. Strains much smaller than 1% can influence surface reconstructions[5,6] and alter epitaxial growth by changing energy barriers for adatom diffusion.[7,8] A limiting factor in experiments has been the inability to control the surface strain in the substrate systematically. Conventionally, strained surfaces are produced using semiconductor[9,10] or metal[11] heteroepitaxial layers. Both pseudomorphic and relaxed thin films, however, are inevitably structurally more complicated than the free surface of a crystal because of dislocations and other defects.[12] Furthermore, the magnitude and symmetry of the possible surface strains are limited by the available thin-film materials. To enable more detailed studies we have fabricated and characterized micromechanical structures on SOI substrates with well-defined surface strains. A key aspect of the use of these structures is the quantitative evaluation of the strain at the surface. We have calibrated the fabrication process using synchrotron x-ray microdiffraction, a technique that allows the local bending and lattice distortion to be measured with submicron spatial resolution.

The micromachined SOI substrates are designed to have a locally strained Si template layer adjacent to areas that remain unstrained. Localized strains are advantageous for isolating the effects of strain on epitaxial growth because they allow for the side-by-side comparison of strained and unstrained surfaces. The symmetry and crystallographic direction of the strain can be modified by changing the geometry of the structure. We have constructed several geometries of these structures and induced a permanent static strain in them with a stressed nonstoichiometric silicon nitride thin film (Fig. 1).

When we perform Ge epitaxial growth studies on these Si (001) strained structures, we find an enhancement in the surface diffusion of Ge in comparison with Ge on unstrained Si. The detailed results of the study of the diffusion of Ge on the surface of a strained bridge structure [Fig. 1(d)] will be reported separately.[13] Briefly, the diffusion studies are of interest because two qualitatively different predictions have resulted from theoretical considerations of the effect of substrate strain on the surface diffusion of Ge on Si.[14,15] These studies differ in their predictions of the dependence of the activation barrier for adatom diffusion on the magnitude of the strain and in the relative shift of the diffusion barriers for Ge and Si adatoms when strain is introduced.

To understand the diffusion observations quantitatively, we determined the absolute magnitude of the distortion of the lattice in the strained areas using synchrotron x-ray mi-

[a]Electronic mail: evans@engr.wisc.edu
[b]Present address: VEECO Instruments, Santa Barbara, CA.
[c]Present address: School of Electrical and Computer Engineering, Cornell University, Ithaca, NY 14853.

 

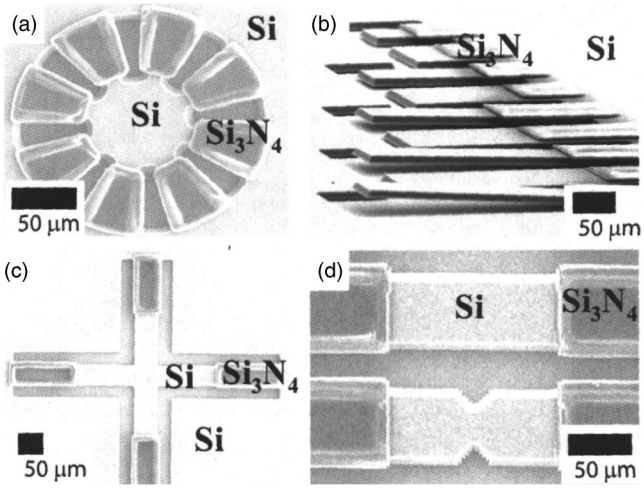


FIG. 1. Scanning electron micrographs of microfabricated strained silicon substrates for epitaxial growth. The silicon nitride thin film stressing the template layer is visible as raised regions. The areas labeled as Si refer to the SOI template layer.

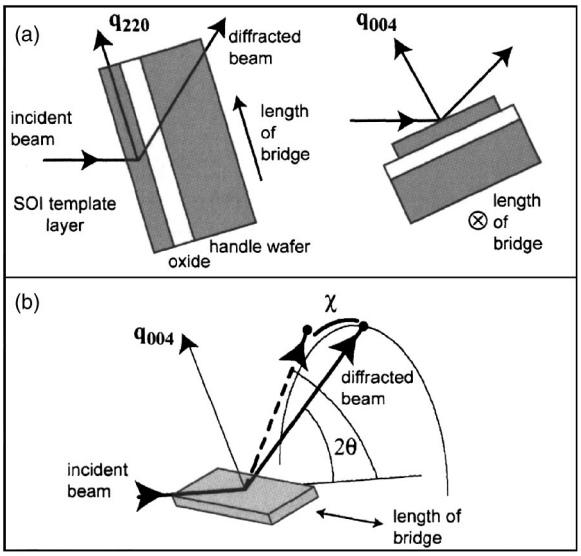


FIG. 2. (a) Synchrotron x-ray microdiffraction measurements of the strain and bending in the bridge structure used a reflection geometry for the (004) x-ray reflection and a transmission geometry for the (220) reflection. (b) A rotation of the (004) planes rotates the x-ray reflection through an angle $\chi$. A change in the lattice spacing can change the $2\theta$ angle of the reflection.

crodiffraction. With this approach it is possible to make direct measurements of micromachined structures with submicron lateral spatial resolution and to resolve strains as small as $10^{-5}$. Other measurements of strain in micromechanical systems have typically been based on either optical or x-ray diffraction[16] measurements of wafer curvature, optical interferometry measurements of the displacement due to strain, photoluminescence,[17] or Raman spectroscopy.[18] In comparison, x-ray microdiffraction couples directly to the silicon lattice spacing and does not require calibration of optical effects with known strains.

## II. EXPERIMENTAL PROCEDURE

The structures shown in Fig. 1 were fabricated on a SOI wafer consisting of a (001)-oriented handle wafer bonded through a $SiO_2$ layer to a 9-$\mu$m-thick crystalline Si (001) template layer. A 1-$\mu$m-thick silicon nitride film was deposited by low-pressure chemical-vapor deposition under conditions producing tensile stress in the film. The stoichiometry and thickness of the nitride layer can be adjusted to tune the force induced into the template layer. The average stress in layers deposited under identical conditions to those used in the fabrication of the freestanding structures was found from wafer curvature measurements on blanket films to be 230 MPa. Exposure to hydrofluoric acid during the release step can unintentionally etch the silicon nitride layer and lead to uncertainties in the stress applied to the final microfabricated structure. In addition exposing the entire structure to elevated temperature during the Ge growth process can reduce the built-in stress in the silicon nitride layer.

X-ray microdiffraction measurements of the bending and strain in the bridge structure were performed at station 2ID-D of the Advanced Photon Source at Argonne National Laboratory.[19] An 11.3-keV incident x-ray beam was focused with a Fresnel zone plate to a spot of 0.3-$\mu$m full width at half maximum in diameter. The focusing optics introduce a beam divergence of 0.05°. The absorption of x-rays by Si is negligible on the length scale of the thickness of the SOI template layer, making x-ray measurements averages over the thickness of the structure. The focal point of the x-ray beam was aligned with the center of an x-ray diffractometer to allow precise diffraction measurements. Diffracted x rays were collected with a charge-coupled device (CCD) camera that allowed measurements of the angular position, angular width, and intensity of x-ray reflections. A slight misalignment of the SOI template layer with respect to the handle wafer both in miscut and in azimuthal orientations allowed the bridge to be distinguished from the handle wafer in x-ray microdiffraction measurements. Such orientation differences are typical of bonded SOI structures.

We have focused, in particular, on characterizing the notched bridge structure [Fig. 1(d)]. The bridge was oriented with the in-plane [110] direction along its length. The total length of the bridge is 510 $\mu$m with the silicon nitride stressor thin film covering all but the central 155 $\mu$m.

## III. RESULTS AND DISCUSSIONS

As expected from the tensile stress in the silicon nitride film and from the upward bending of the cantilever structures [Fig. 1(b)], the bridge bent upwards away from the handle wafer. The bowing of the bridge rotates the silicon lattice planes and shifts the angular positions of x-ray reflections. We have performed two independent measurements of this effect to quantify the bending of the bridge using the x-ray diffraction strategies shown in Fig. 2(a). Relative to the reflection from an undistorted region, the reflections from strained silicon can appear at a different $2\theta$ angle or can be rotated to a new position on the Si powder circle due to bending. These effects are illustrated in Fig. 2(b). Rocking curves for the Si (220) reflection were acquired by rotating the sample normal within the diffraction plane. The measurements were collected at a series of points along the length of the bridge with the beam approximately at the midpoint of its

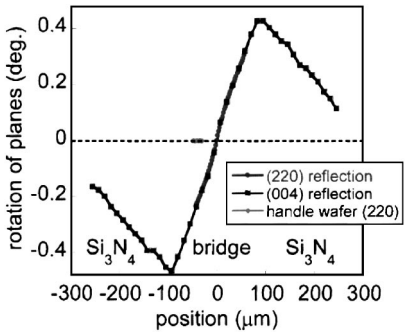


FIG. 3. The misorientation of Si (220) planes as a function of position along the bridge measured using x-ray microdiffraction in a transmission geometry (circles). Measurements using the surface-normal (004) reflection (squares) show the same trend across the exposed portion of the bridge and a reversal in the curvature under the silicon nitride stressor. The orientation of the handle wafer (220) planes is independent of position (diamonds).

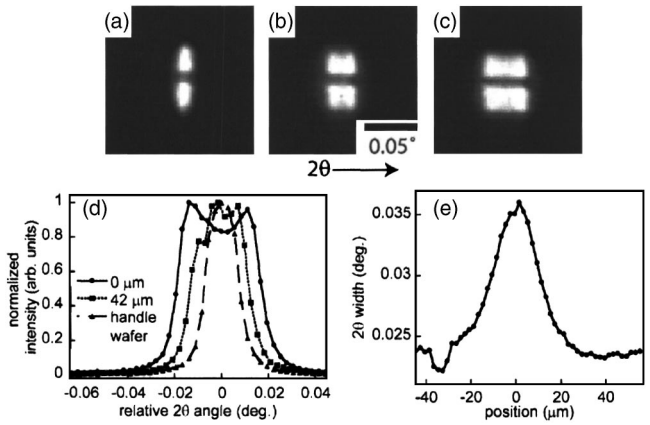


FIG. 4. The angular width of the Si (220) diffraction spot in the direction of the conventional $2\theta$ angle depends on the position of the x-ray beam along the bridge. The handle wafer reflection (a) serves as a benchmark. The x-ray reflections from the bridge, both at 42 $\mu$m from the notch and at the notch, (b) and (c), respectively, are broadened in the $2\theta$ direction due to the variation of the (220) spacing through the thickness of the bridge. The width of the (220) x-ray reflection varies along the length of the bridge, (d), and reaches a maximum at the notch (e). The dip at −35 $\mu$m is an artifact arising from the coincidental alignment of handle wafer and bridge reflections at that location.

width. The (220) x-ray reflection corresponds to diffraction from planes of atoms with normals nearly along the direction of the bridge. The reflections from (220) planes were observed in a diffraction geometry in which the x-ray beam passed through the entire thickness of the bridge and handle wafer. The center of the Si (220) rocking curve shifted by nearly 0.5° across the central 100-$\mu$m length of the span of the bridge due to bending of the bridge along its length. The angular deviation was nearly proportional to the distance from the midpoint of the length of the bridge, but varied more rapidly near the notch.

A second, independent, observation of the bending was obtained by orienting the long axis of the bridge perpendicular to the diffraction plane and measuring the angle $\chi$ between the undistorted Si (004) diffraction spot and the spot produced the by Si (004) planes in the bent part of the bridge. For small distortions, the tilting of the planes is a factor of $k/q_{004} \approx 1.24$ larger than $\chi$, the angular separation of the spots. Here $k$ is the magnitude of the incident x-ray wave vector and $q_{004}$ is the spatial frequency associated with the (004) reflection from Si. The measurements of the (004) reflection were conducted across the full length of the exposed Si bridge and also included regions at the ends of the bridge that were covered by the silicon nitride stressor layer. The total angular deviation across the exposed portion of the bridge exceeded 0.8°. The curvature of the bridge in the regions covered by the silicon nitride stressors was in the opposite direction to the curvature in the uncovered central area of the bridge.

The observations of the bending using these two x-ray reflections are plotted together in Fig. 3. As a benchmark for the curvature, we can compare reflections from the bridge with those from the handle wafer. There is no variation of the rocking-curve angle of the (004) reflection of the handle wafer with position. Integrating the angle through which the x-ray reflections from the bridge are tilted, we found that the total upward displacement at the center of the bridge is 1.3 $\mu$m. The radius of curvature of the bent bridge can be found from the rate of change of the rocking-curve angle with position. The radius of curvature is smaller in the region of the notch, where it reaches a minimum of 1 cm.

The lattice distortion in the bridge can also be found directly by examining the $2\theta$ angles to which the x-ray beam is diffracted. Images of the diffraction spot produced by the (220) reflection were acquired using the CCD detector and are shown in Fig. 4. In these images the horizontal direction corresponds to the conventional $2\theta$ angle of x-ray diffraction as defined in Fig. 2(b). The horizontal stripe at the center of the diffracted beams is the shadow of the center stop used in the x-ray focusing apparatus.[19] The $2\theta$ angles to which the x-rays are reflected from (220) planes depend on the lattice spacings of these planes. The bending of the bridge changes the (220) spacing because a fixed number of Si planes must cover a changed total length at the surfaces of the bridge. The width in the $2\theta$ direction of the (220) diffraction spot of the undistorted handle wafer [Fig. 4(a)] is 0.02° and serves as a reference to which the reflections from the distorted regions can be compared. The reflections from the bridge [Figs. 4(b) and 4(c)] are significantly broader than the handle wafer reflection. The integrated intensity of these diffraction spots is plotted in Fig. 4(d). The width of the reflections depends on the degree of strain in the template layer and exceeds 0.035° at the position of the notch [Fig. 4(e)]. This broadening is symmetric about the original $2\theta$ angle of the (220) reflection and represents a spread of lattice constants through the thickness of the bridge. The CCD images also record the intensity as a function of the angular direction perpendicular to $2\theta$, which appears as the vertical direction in the images shown in Fig. 4. The width of the images of the reflections in this direction is set by the divergence of the focused beam.

The strain along the [220] direction in the Si bridge can be estimated in two ways. From the radius of curvature, the difference in the uniaxial strain between the top and bottom of the bridge at the notch is $\varepsilon_{\text{top}}$-$\varepsilon_{\text{bottom}} = t/R$, where $t = 9$ $\mu$m is the thickness of the Si layer from which the bridge is formed and $R$ is the radius of curvature. This expression is based on the approximation that none of the elastic strain

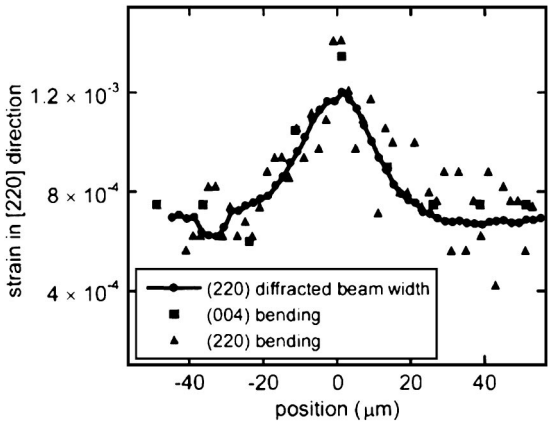


FIG. 5. Estimates of the strain derived from the bending of the bridge and from the excess angular width of the diffraction spot.

that would arise due to bending is relaxed by the formation of structural defects. It is possible to make an independent estimate of the strain from the angular width of the x-ray reflections without the approximation that the bending is purely elastic. The degree to which strain broadens the (220) reflection can be found by assuming that the intrinsic width of the handle wafer reflection, limited by instrumental resolution, adds in quadrature with the excess width arising from the gradient of lattice constants through the thickness of the bridge. These two estimates of the strain agree very well and are shown together in Fig. 5. The strain difference between the top and bottom of the bridge exceeds $1\times10^{-3}$ at its maximum at the notch.

The upward bending of the Si bridge is consistent with our observations of similar cantilevered beams [Fig. 1(b)]. The stress induced by the silicon nitride layer leads to a torque on the beam and causes it to deflect away from the handle wafer. The expected bending can be estimated using x-ray microdiffraction measurements of the curvature of the region of the Si template layer *beneath* the silicon nitride thin film. In a scan across the width of the bridge in an area covered by the silicon nitride we found that the template layer underneath the silicon nitride stressor is bent to a radius of curvature of 1.3 cm. Assuming a negligible stress at the bottom surface of the Si bridge, and applying the relationship between stress and bending applicable to infinite isotropic thin films,[16,20] the average stress in the silicon nitride film is 190 MPa. This is 15% less than we observed in the blanket films, which could in part be due to uncertainty in the nitride layer thickness following the processing of the bridge. In the area beneath the nitride stressors, the radius of curvature of the template layer in the direction along the bridge, however, is approximately a factor of 2 greater than in the direction across the bridge. Thus, to within a factor of 2 accuracy in the radius of curvature, a qualitative rationalization of the total bending of the notched bridge is to imagine that the notched Si bridge connects two cantilevers raised from the plane of the surface by the silicon nitride stressor layers.

An additional source of strain must also be considered. Because the ends of the bridge are fixed, the total length of the bent bridge is slightly longer than an undistorted bridge. The magnitude of the strain resulting from this effect scales approximately as $2(h^2/l^2)$, where $l$ is the length of the bridge and $h$ is the total vertical deflection. With $h=1.3$ $\mu$m and $l=500$ $\mu$m, this elongation of the bridge leads to a strain of $1.4\times10^{-5}$, a small correction to the strain due directly to bending.

## IV. CONCLUSION

The strain at the surface of the bridge structure has a large effect on the diffusion of Ge adatoms, raising the possibility that the strain generated using micromachining techniques can lead to a degree of control in epitaxial growth.[13] Despite the significant effect of strain we have found in surface thermodynamics and kinetics, the strain at the silicon surfaces in these structures is approximately an order of magnitude lower than the strain typically induced into silicon to optimize electron mobility.[3] With optimized structures at smaller length scales, however, micromachined devices have the potential to lead to large electronic effects in the template layer or in epitaxial thin films. In silicon, a well-defined local strain could lead to a controlled anisotropic distortion of the band structure.[21] Already, strains of the magnitude we have found in the bridge structure are predicted to shift the boundaries between magnetic and dielectric phases of complex oxides.[22] The measurement of the strain in the microstructures using microdiffraction calibrates the fabrication processes, which will lead to designable microstrain inducers.

## ACKNOWLEDGMENTS

This work was supported by the National Science Foundation through the University of Wisconsin Materials Research Science and Engineering Center, Grant No. DMR-0079983. Use of the Advanced Photon Source was supported by the U. S. Department of Energy, Office of Science, Office of Basic Energy Sciences, under Contract No. W-31-109-Eng-38. This work was also partially supported by DARPA-MTO Contract No. F30602-00-2-0572.

[1] T. A. Langdo *et al.*, Appl. Phys. Lett. **82**, 4256 (2003).
[2] G. K. Celler and S. Cristoloveanu, J. Appl. Phys. **93**, 4955 (2003).
[3] F. Schäffler, Semicond. Sci. Technol. **12**, 1515 (1997).
[4] K. Rim *et al.*, Tech. Dig. - Int. Electron Devices Meet. 49 (2003).
[5] F. K. Men, W. E. Packard, and M. B. Webb, Phys. Rev. Lett. **61**, 2469 (1988).
[6] B. S. Swartzentruber, Y. W. Mo, M. B. Webb, and M. G. Lagally, J. Vac. Sci. Technol. A **8**, 210 (1990).
[7] C. Roland and G. H. Gilmer, Phys. Rev. B **46**, 13428 (1992).
[8] D. J. Shu, F. Liu, and X. G. Gong, Phys. Rev. B **64**, 245410 (2001).
[9] E. Zoethout, O. Gürlü, H. J. W. Zandvliet, and B. Poelsma, Surf. Sci. **452**, 247 (2000).
[10] V. Cherepanov and B. Voigländer, Appl. Phys. Lett. **81**, 4745 (2002).
[11] H. Brune *et al.*, Phys. Rev. B **52**, R14380 (1995).
[12] F. Wu, X. Chen, Z. Zhang, and M. G. Lagally, Phys. Rev. Lett. **74**, 574 (1995).
[13] P. P. Rugheimer, C. H. Lee, D. E. Savage, M. M. Roberts, and M. G. Lagally (unpublished).
[14] A. van de Walle, M. Asta, and P. W. Voorhees, Phys. Rev. B **67**, 041308R (2003).
[15] L. Huang, F. Liu, and X. G. Gong, Phys. Rev. B **70**, 155320 (2004).
[16] A. Segmuller, J. Angilelo, and S. J. La Placa, J. Appl. Phys. **51**, 6224 (1980).
[17] A. Borowiec, D. M. Bruce, D. T. Cassidy, and H. K. Haugen, Appl. Phys. Lett. **83**, 225 (2003).
[18] S. Nakashima, T. Yamamoto, A. Ogura, K. Uejima, and T. Yamamoto, Appl. Phys. Lett. **84**, 2533 (2004).

[19]Z. Cai, B. Lai, Y. Xiao, and S. Xu, J. Phys. IV **104**, 17 (2003).
[20]W. A. Brantley, J. Appl. Phys. **44**, 534 (1973).
[21]P. Sutter, E. Mateeva, P. Rugheimer, and M. Lagally, Surf. Sci. **532–535**, 789 (2003).
[22]O. Diéguez, S. Tinte, A. Antons, C. Bungaro, J. B. Neaton, K. M. Rabe, and D. Vanderbilt, Phys. Rev. B **69**, 212101 (2004).